



Asian Journal of Chemistry; Vol. 29, No. 9 (2017), 2057-2064

# ASIAN JOURNAL OF CHEMISTRY

<https://doi.org/10.14233/ajchem.2017.20827>



## Synthesis of Spinel $\text{ZnFe}_2\text{O}_4$ Modified with SDS via Low Temperature Combustion Method and Adsorption Behaviour of Crystal Violet Dye

MUKESH KUMAR, HARMANJIT SINGH DOSANJH and HARMINDER SINGH\*

Department of Chemistry, School of Physical Sciences, Lovely Professional University, Phagwara-144 411, India

\*Corresponding author: Tel: +91 18 24444307; E-mail: [harminder.singh@lpu.co.in](mailto:harminder.singh@lpu.co.in); [harminder\\_env@yahoo.com](mailto:harminder_env@yahoo.com)

Received: 15 April 2017;

Accepted: 30 May 2017;

Published online: 15 July 2017;

AJC-18491

Nano materials such as nano ferrites and their composites have been intensively investigated for water treatment. In present study nano zinc ferrites were successfully synthesized using low temperature combustion method and the surface of nano zinc ferrite was modified with surfactant sodium dodecyl sulphate (SDS). The characterization and morphology of zinc ferrite have been studied by FTIR, SEM and XRD techniques. Sodium dodecyl sulphate modified zinc ferrite showed excellent adsorption behaviour toward crystal violet dye. The adsorption behaviour has been studied at various parameters such as pH, adsorbent dose, temperature, concentration and time. The experimental data obtained from adsorption studies have been analyzed by Langmuir, Freundlich, Temkin and D-R adsorption isotherm models at different temperatures. The data was well fitted in Langmuir isotherm model. The maximum adsorption capacity ( $Q_0$ ) at different temperatures as 298, 303 and 308 K were 135.5, 170.6 and 188.3 mg/g. The adsorption kinetics was studied by using pseudo first order, pseudo second order and intra particle diffusion model. The adsorption kinetics was found to follow the pseudo second order kinetic model. Adsorption thermodynamic parameters  $\Delta G^\circ$ ,  $\Delta H^\circ$  and  $\Delta S^\circ$  have been calculated from experimental data and indicated that the adsorption process was spontaneous in nature. The results showed that SDS-Zn ferrites as a magnetic adsorbent might be a suitable alternative to remove dyes from waste water.

**Keywords:** Spinel Zn ferrite, Low temperature combustion method, Surface modification, Adsorption Kinetics, Adsorption isotherm.

### INTRODUCTION

Dyes are main contributor of water pollution in many industries such as paper, leather, textile *etc.* The removal of dyes from the polluted water is one the matter of most concern. This is because most of dyes are toxic, carcinogenic and mutagenic in nature and the removal of such dyes from aquatic systems is extremely important from the environmental view point. Mostly dyes are organic compounds having aromatic complex structure and difficult to remove from polluted water [1,2]. From last four decades, different techniques such as coagulation, advance oxidation, membrane filtration, reverse osmosis and adsorption [3-8] have been used to remove dyes from polluted water. Literature studies reveal that among these methods adsorption technique is one of most convenient technique for the removal of dyes from waste water. Adsorption method has various advantages over the conventional methods such as simple, low cost and less land involvement [7,8]. In adsorption process various types of natural and synthetic adsorbents such as activated carbon, clay, clay minerals, rice husk, saw dust, *etc.* [9-16] have been used as natural and synthetic adsorbents for waste water treatment. From last two

decades, the use of nano particles in adsorption field is getting more interest. Literature studies indicate that nano materials have high adsorption capacity [17-23] in comparison to traditional adsorbents and can be prove as an excellent adsorbent to remove dyes from waste water. However, being smaller in size and such particles cannot be recovered efficiently from treated water by using traditional methods such as filtration, sedimentation *etc.* The use of magnetic nano ferrites as adsorbent in waste water treatment can overcome the problems and be readily separated from treated water by applying external magnetic field. Nano ferrites have high adsorption capacity to remove dyes from waste water [24-28]. These types of nano particles have highly reactive surface with less stability in general environmental conditions. Therefore various surface modification techniques like doping of metal/metal oxides, polymer coating and surfactant coating have used to modify the surface of nanoferrites [29]. Recent studies revealed that the surface modified nano ferrites have high stability and adsorption capacity to remove dyes from waste water [30-49]. Surface modification is essential need to enhance the adsorption capacity and stability of nano ferrites. In present study, magnetically separable nano zinc ferrites (ZFN) was synthesized

by using low temperature combustion method and its surface was modified with sodium dodecyl sulphate (SDS). The adsorption behaviour of SDS modified zinc ferrite (ZFN-SDS) was studied with crystal violet dye.

## EXPERIMENTAL

For the synthesis of zinc ferrites, all the chemical reagents were of analytical grade and used as received without further purification. Zinc nitrate, ferric chloride, hydrazine hydride, diethyl oxalate and sodium dodecyl sulphate were obtained from Loba Chemie Reagent Co. Ltd. and crystal violet was obtained from Quallkems.

**Synthesis of Zn ferrite:** For zinc ferrites synthesis by low temperature combustion method, stoichiometric quantities of AR grade zinc nitrate and ferric nitrate were thoroughly mixed in beaker and the reaction mixture was concentrated on water bath with small addition of oxalyldihydrazide (ODH) as organic fuel. The decomposition of oxalyldihydrazide into reaction mixture involved exothermic reaction in nature. The released energy helped in decomposition of solution into desired products at faster rate. The gel solution was then transferred to crucible and combusted at 600 °C for 6 h in muffle furnace. The brown powder obtained was desired product of nano zinc ferrite [48].

**Surface modification of zinc ferrite with SDS:** To modify the surface of above prepared ZFN with SDS (sodium dodecyl sulphate), an aqueous solution of 0.07 M SDS was added to 12 % aqueous solution of zinc ferrite. The mixture solution was constantly stirred for approximately 3 h at 200 rpm. The surfactant coated zinc ferrites were separated from the mixture solution by filtration and dried at 40 °C.

**Characterization:** The surface characterization of uncoated ZFN and modified ZFN-SDS coated were carried out by using FT-IR spectrophotometer (Shimadzu-8400) in range of 4000-400  $\text{cm}^{-1}$  and surface morphological structure of nano material was examined by X-ray diffraction (XRD, Philips) and scanning electron microscope (SEM-JEOL 6100) was done to confirm the formation of desired product.

**Adsorption studies:** Batch adsorption process was used to study the adsorption behaviour of crystal violet dye with modified ZFN-SDS. In this process, the effect of various parameters like pH, contact time, adsorbent dose, adsorbate concentration and effect of different temperatures were studied. For this aqueous solution of known concentration of crystal violet and known mass of adsorbent was taken in 250 mL conical flasks and kept in thermostatic shaker at 125 rpm for 3 h at a fixed temperature. The sample was withdrawn and centrifuged at 2000 rpm. The reduced concentration of sample was measured by measuring the absorbance in UV-spectrophotometer (Shimadzu, UV 1800) at 591 nm.

Initial studies to compare the adsorption behaviour of ZFN and ZFN-SDS were performed and it was found that the ZFN had only 27 % removal efficiency for crystal violet dye while in case of ZFN-SDS was 85 % removal efficiency.

The adsorption capacity ( $Q_e$ ) in mg/g and percentage removal of dye was calculated by following equation as:

$$Q_e = \frac{(C_o - C_e) \cdot V}{m} \quad (1)$$

$$\text{Removal (\%)} = \frac{(C_o - C_t)}{C_o} \times 100 \quad (2)$$

where  $C_o$ ,  $C_t$  and  $C_e$  are the initial, at time  $t$  and equilibrium concentrations (in mg/L) of adsorbate,  $V$  is the volume of the dye solution (L) and  $m$  is the mass of adsorbent used (g).

## RESULTS AND DISCUSSION

### Surface characterization and morphological studies of ZFN and ZFN-SDS composites

**FT-IR spectroscopy:** FTIR spectra of zinc ferrite nanoparticles was obtained for the detection of the functional group in between the range 4000-400  $\text{cm}^{-1}$ . FT-IR spectrum of zinc ferrite shows two distinct absorption peaks below 600  $\text{cm}^{-1}$  in both of spectra of ZFN and ZFN-SDS which represented the tetrahedral and octahedral sites of spinel structure of zinc ferrite (Fig. 1). In Fig. 1, ZFN-SDS spectra there was a band of peaks at about 3400, 2950, 2850, 1630, 1435  $\text{cm}^{-1}$  observed due to O-H stretching vibration, C-H asymmetric stretching, C-H symmetrical stretching, the bending vibration of observed molecular water and bending vibration of C-H. The peaks at 1384-874  $\text{cm}^{-1}$  are due to asymmetric and symmetric stretching and bending of the  $\text{SO}_4^{2-}$  anion or  $\text{CH}_3$  bending,  $\text{CH}_2$  bending and C-C stretching mode of sodium dodecyl sulfate [50].

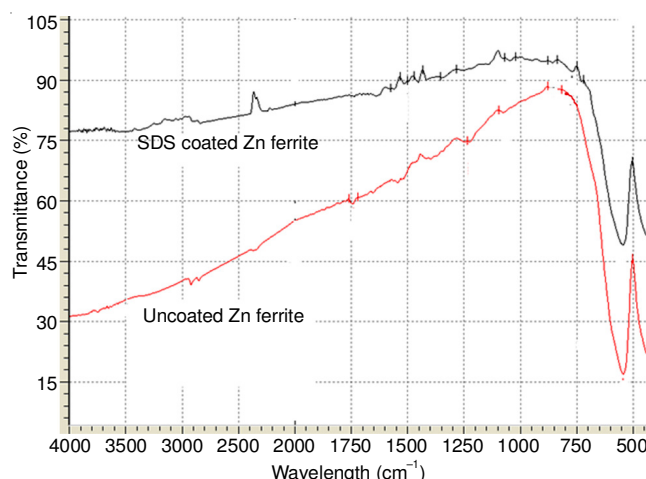


Fig. 1. FTIR overlay image of uncoated Zn ferrite and SDS coated Zn ferrite

**X-ray diffraction:** Crystallization of materials was studied by X-ray diffraction (XRD) and Fig. 2 represents the XRD pattern of ZFN and ZFN-SDS composite. The most intense peak (311) and Miller indices (220), (222), (400), (422), (511) and (440) matched well with the general peaks of ZFN [50]. These peaks indicated that spinel ZFN have been formed. Besides these peaks, there were few peaks observed which represented the formation of impurities  $\text{Fe}_2\text{O}_3$  in ZFN and modified ZFN-SDS. The average crystalline size of ZFN and ZFN-SDS composite was calculated by using Secherer formula as shown below:

$$D = \frac{0.89\lambda}{\beta \cos \theta} \quad (3)$$

where  $D$  is the crystalline size,  $\lambda$  is the X-ray wavelength,  $\beta$  is the broadening peak and  $\theta$  is the diffraction angle for maximum

peak. The calculated crystalline size of ZFN and SDS-ZFN varies between 24 nm to 78 nm. The calculated average crystalline size of ZFN and SDS-ZFN were below 80 nm. The intense peaks indicated the good crystallinity of both the compounds. The XRD pattern of ZFN and SDS-ZFN has shown in Fig. 2(a,b).

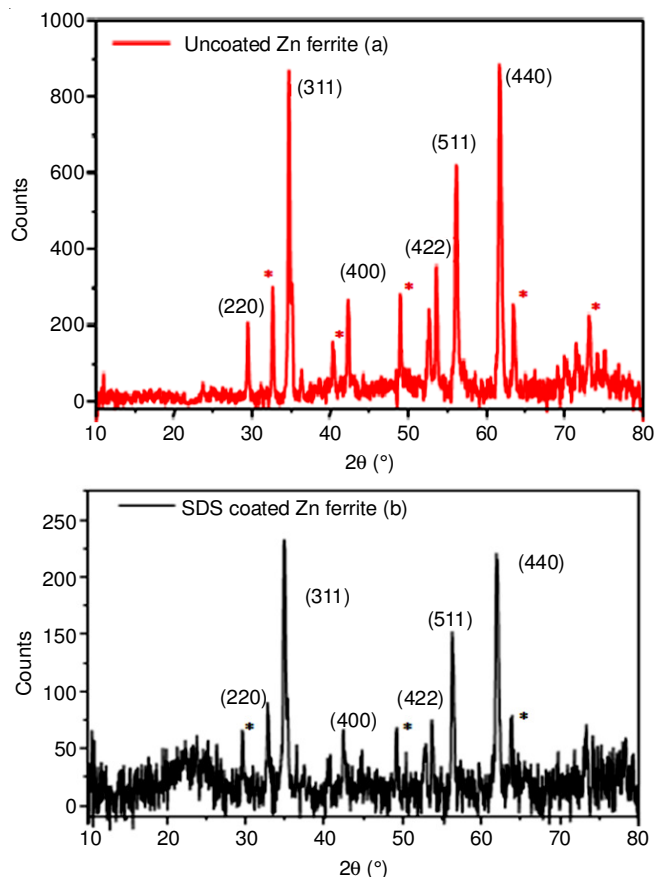


Fig. 2. (a) XRD pattern of uncoated Zn ferrite and (b) after SDS coated Zn ferrite

**SEM images:** In order to visualize the surface of nano ferrite before and after coating SEM images are obtained as shown in Fig. 3(a,b). Particles formed agglomeration and irregular agglomeration is observed.

#### Adsorption studies of crystal violet on SDS modified Zn ferrites

**Effect of contact time:** Adsorption is a time dependent process and directly influenced by contact time. To study the effect of time on adsorption behaviour of ZFN-SDS, known concentration and volume of the dye solution was kept in contact with adsorbent in thermostatic shaker. An aliquot of the sample was removed after fixed time interval and residual dye concentration was analyzed. With the increase in contact time the adsorption also increased and a stage came when it reached at equilibrium. Fig. 4 indicated that at initial stage the removal efficiency of dye was 35 % and with time it increased upto 85 %. At initial stage large number of vacant sites are available on the surface of adsorbent and dye molecules are attached to these sites. At certain stage these sites were totally occupied and equilibrium condition achieved between the adsorbate and adsorbent molecules [48].

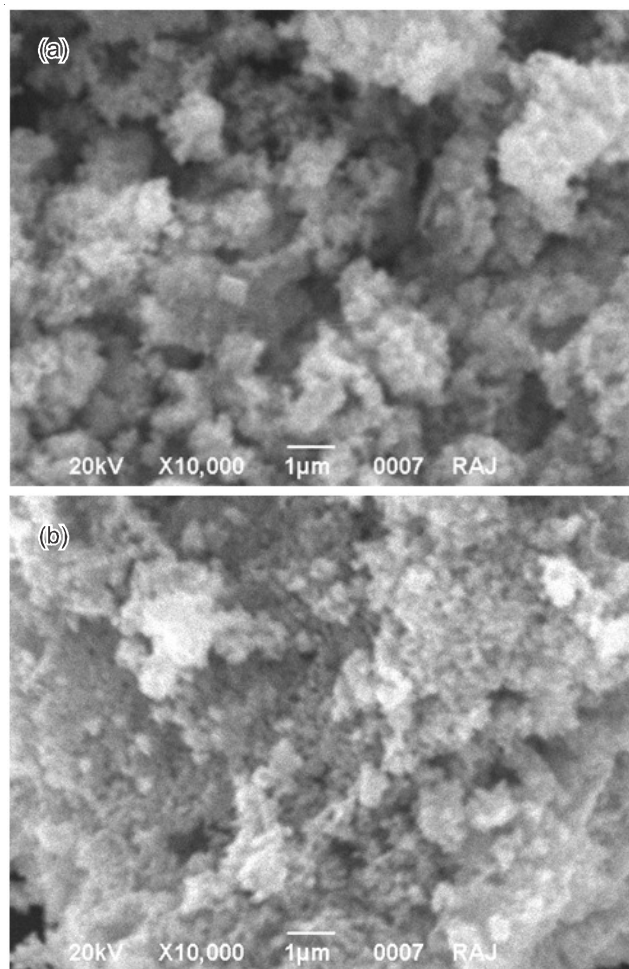


Fig. 3. (a) SEM image of uncoated Zn ferrite, (b) SEM image of SDS coated Zn ferrite

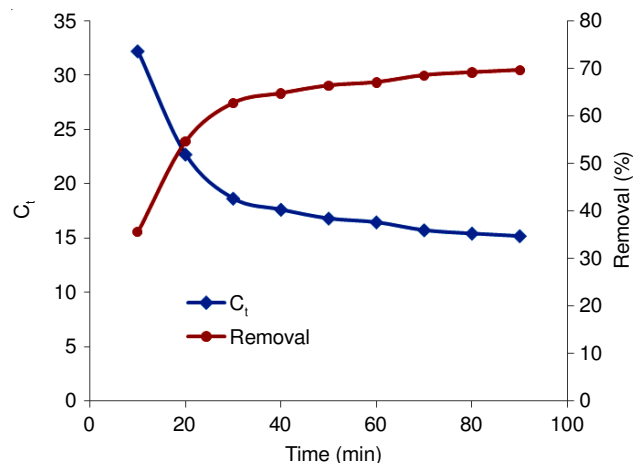


Fig. 4. Effect of contact time on removal % of crystal violet dye with SDS coated zinc ferrite

**Effect of pH:** The pH of adsorbate solution directly influence the dye removal ability of adsorbate. It affects the stability and colour intensity of adsorbate solution. Therefore pH is significant controlling feature in adsorption process. The adsorption of crystal violet dye on the surface of ZFN-SDS was studied at different pH values. To determine the optimum pH of solution, the pH value was changed from 2-10 with fixed initial concentration of crystal violet dye (50 mg/L) and



contact time 3 h. The effect of pH on the removal of crystal violet is given in Fig. 5. It was observed that as pH of solution increases the dye removal efficiency also increased consistently and reached maximum at pH about 6-7 and then further decreased. The SDS is anionic in nature due to that reason the electrostatic attraction was low at lower pH. The extent of adsorption increased with pH because surface charge density decreases due to which electrostatic attraction between the adsorbent and the crystal violet dye also increase and it was maximum at neutral pH [48]. Thus there exist maximum attraction between the negatively charged surface of the adsorbent and positively charged cationic dye molecule at pH about 7, which favours adsorption of crystal violet dye upto 85 %.

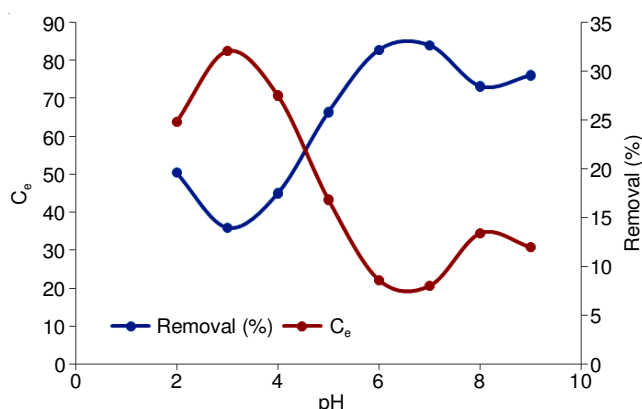


Fig. 5. Effect of pH on the removal % of crystal violet dye with SDS coated Zn ferrite

**Effect of adsorbent dosage:** Effect of adsorbent dose was studied with ZFN-SDS for the removal of crystal violet dye from solution. The adsorbent dose varied from 0.1 to 0.5 g with constant concentration 50 mg/L. From Fig. 6 it is evident that the removal efficiency of the dye was increased upto 96 % with increase in the adsorbent dose. With increase in the adsorbent dose, the vacant sites for adsorption increases which was responsible for the increase in removal efficiency of the dye [40,48].

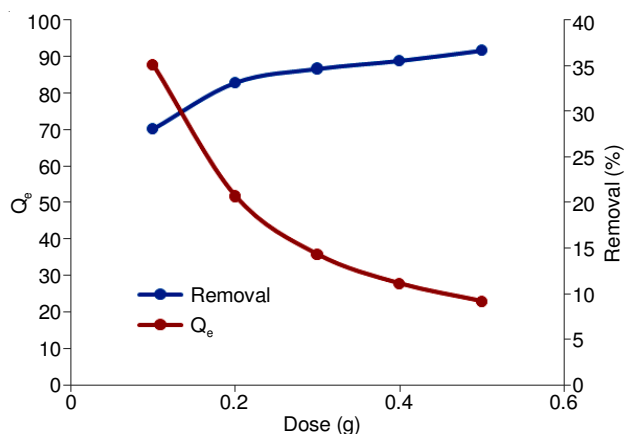


Fig. 6. Effect of dosing on removal % of crystal violet dye with SDS coated Zn ferrite

**Effect of concentration:** The effect of concentration on the adsorption of crystal violet was studied and result is shown in Fig. 7. The adsorption capacity of crystal violet dye increased

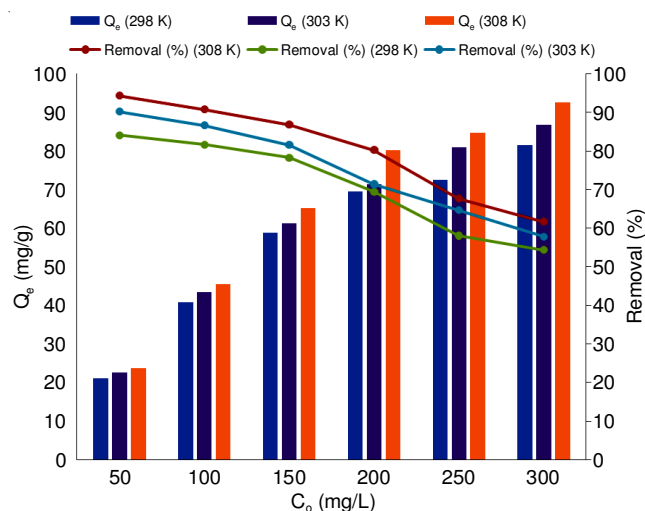


Fig. 7. Effect of concentration on the removal % of crystal violet dye with SDS coated Zn ferrite

with increase in dye concentration. This increase in adsorption capacity may be due to higher interaction between adsorbate and adsorbent molecules. On the other hand percentage removal of crystal violet dye was decreased with increase in the concentration of crystal violet dye. It may be due to decrease in available active sites with increase in dye concentration. This study was conducted at different temperature ranges as 298, 303 and 308 K to observe the effect of temperature. It was observed that with increase in temperature adsorption of dye also increased and it indicated that adsorption process was endothermic in nature [48].

**Adsorption kinetics:** Different adsorption kinetic models such as Lagergren pseudo first order, pseudo second order and Elovich kinetic models were used to study the adsorption kinetics of ZFN-SDS and the data obtained was correlated with different models.

The experimental data obtained in this study was fitted in different adsorption kinetic models and plots are represented in Fig. 8(a-b). The values of various constants related with these kinetic models were calculated using these plots and are represented in Table-1. The experimental data represented that the correlation coefficients of the pseudo second order kinetic model ( $R^2 > 0.99$ ) was greater than that of pseudo first order model and Elovich model. It showed that the adsorption fits

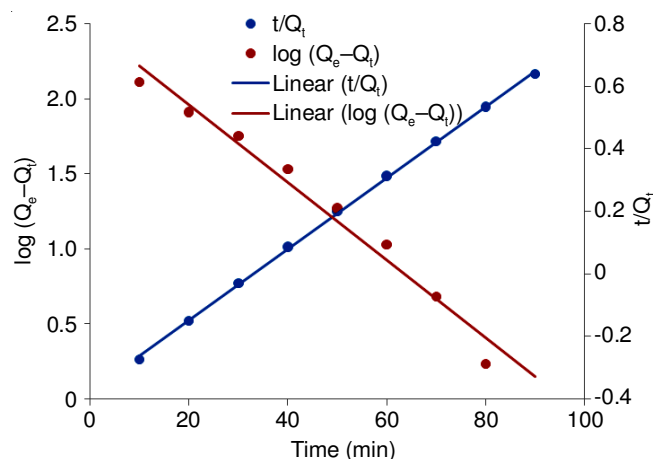


Fig. 8a. Lagergren pseudo first order and pseudo second order kinetic model

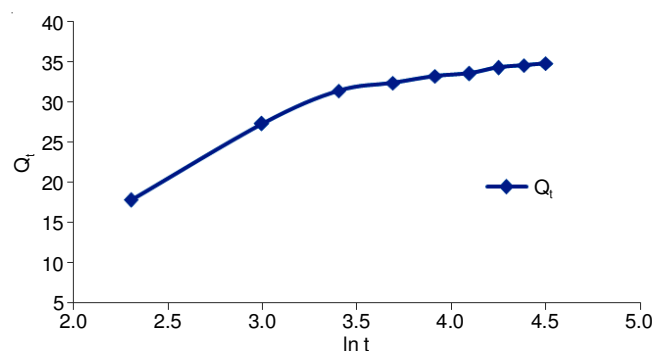


Fig. 8b. Elovich model of adsorption kinetics of SDS coated Zn ferrite

TABLE-1 CALCULATED VALUES OF DIFFERENT ADSORPTION KINETIC MODELS WITH LINEAR FORM			
Adsorption kinetics model	Linear form	Constant	Calculated values
Lagergren pseudo first order	$\log(Q_e - Q_t) = \log Q_e - \frac{K_1}{2.303} t$	$Q_e$ $K_1$ $R^2$ $SD$	24.386 0.055 0.976 0.100
Lagergren pseudo second kinetic model	$\frac{1}{Q_t} = \frac{1}{K_2 t Q_{e2}} + \frac{t}{Q_e}$	$Q_e$ $H$ $K_2$ $R^2$ $SD$	38.53600 4.38400 0.00295 0.99900 0.03800
Elovich model	$Q_t = \frac{1}{\beta} \ln \alpha \beta + \frac{1}{\beta} \ln t$	$A$ $B$ $R^2$ $SD$	13.052 0.139 0.889 1.974

to pseudo second order better than pseudo first order kinetic model [40,48].

Beside kinetic models, to study the intra particle diffusion behaviour of adsorbent, Weber and Morris intra-particle diffusion model was applied to analyze the kinetic data to explain the mechanism of diffusion. The data was fitted in Weber Morris model and the plot obtained was not linear in shape and clarify that intra-particle diffusion was not rate determining step in the adsorption study (Fig. 9). It also clarify that the adsorption process was not follow diffusion method during adsorption [48].

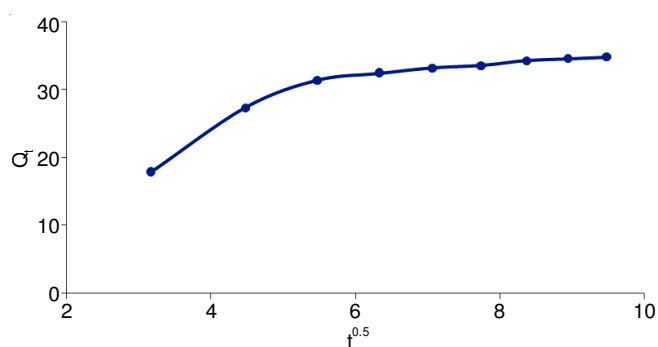


Fig. 9. Weber Morris model of adsorption study

**Adsorption isotherm:** Adsorption isotherms describe the equilibrium of the adsorption of the adsorbate material at the surface of adsorbent at constant temperature. Different types

of adsorption isotherm models are used to describe the adsorption equilibrium. In this study Langmuir, Freundlich, Temkin and Dubinin-Raduskevich (D-R) isotherms were used to describe the equilibrium of adsorption of crystal violet on ZFN-SDS surface at three different temperatures as 298-308 K. The equilibrium data obtained is represented in Fig. 10(a-d) [48]. The equations, values of various constants related with these isotherms were calculated using these plots and represented in Table-2. The values of correlation coefficient ( $R^2$ ) for Langmuir model was observed to be highest followed by Temkin, Freundlich and Dubinin-Raduskevich (D-R) adsorption models which indicated that experimental data fitted well to Langmuir model than other models. This may be due to the fact that SDS-modified adsorbent has homogeneous distribution of active sites and same is the assumption of Langmuir model. Langmuir model is also based on the assumptions that the adsorption is a reversible process and adsorption is because of mono layered molecules. From Table-2 it was found that the maximum adsorption capacities obtained by Langmuir isotherm were 135 mg/g, 170.6 mg/g and 188 mg/g at different temperatures as 298, 303 and 308 K. It is clear from this data that as temperature increased adsorption capacity also increased so this can be termed as endothermic process. Also the value of  $E$  (from D-R adsorption isotherm) was found above 100 KJ/mol which represented that the adsorption process may be chemisorptions in nature [48].

**Adsorption thermodynamics:** Adsorption thermodynamics represent the temperature effect on the adsorption behaviour of adsorbent. Different thermodynamic variables such as enthalpy change ( $\Delta H^\circ$ ), free energy change ( $\Delta G^\circ$ ), entropy change ( $\Delta S^\circ$ ) and equilibrium constant ( $K_d$ ) can be calculated using vant Hoff equation which is represented as:

$$\Delta G^\circ = Rt \ln K_d \quad (4)$$

as per thermodynamics  $\Delta G^\circ$  is represented by relationship between  $\Delta S^\circ$  and  $\Delta H^\circ$  as shown in equation:

$$\Delta G^\circ = \Delta H^\circ - T\Delta S^\circ \quad (5)$$

As joining eqns. 4 and 5, we get:

$$\ln K_d = \frac{\Delta S^\circ}{R} - \frac{\Delta H^\circ}{RT} \quad (6)$$

where  $K_d$  = Langmuir equilibrium constant.

The different types of thermodynamic variables such as enthalpy change ( $\Delta H^\circ$ ), free energy change ( $\Delta G^\circ$ ), entropy change ( $\Delta S^\circ$ ) and equilibrium constant ( $K_d$ ) were calculated from the linear plot of  $\ln K_d$  versus  $1/T$  (Fig. 11). Effect of temperature on the removal of crystal violet dye with ZFN-SDS was investigated at different temperature ranges as 298-308 K by keeping other experimental conditions constant. It was observed that the crystal violet removal increased with increase in temperature. It was supposed that on increasing solution temperature some of pores enlarged which result increase in surface area [48] available for adsorption of crystal violet. Table-3 represented the calculated values of thermodynamic parameters for crystal violet with ZFN-SDS. The positive  $\Delta H^\circ$  values confirmed the endothermic nature of adsorption process. The  $\Delta H^\circ$  values were in the range of 23-88 kJ/mol which showed the nature of adsorption process was endothermic. The positive values of  $\Delta H^\circ$  and  $\Delta S^\circ$  were also indicate the affinity of crystal violet towards ZFN-SDS.

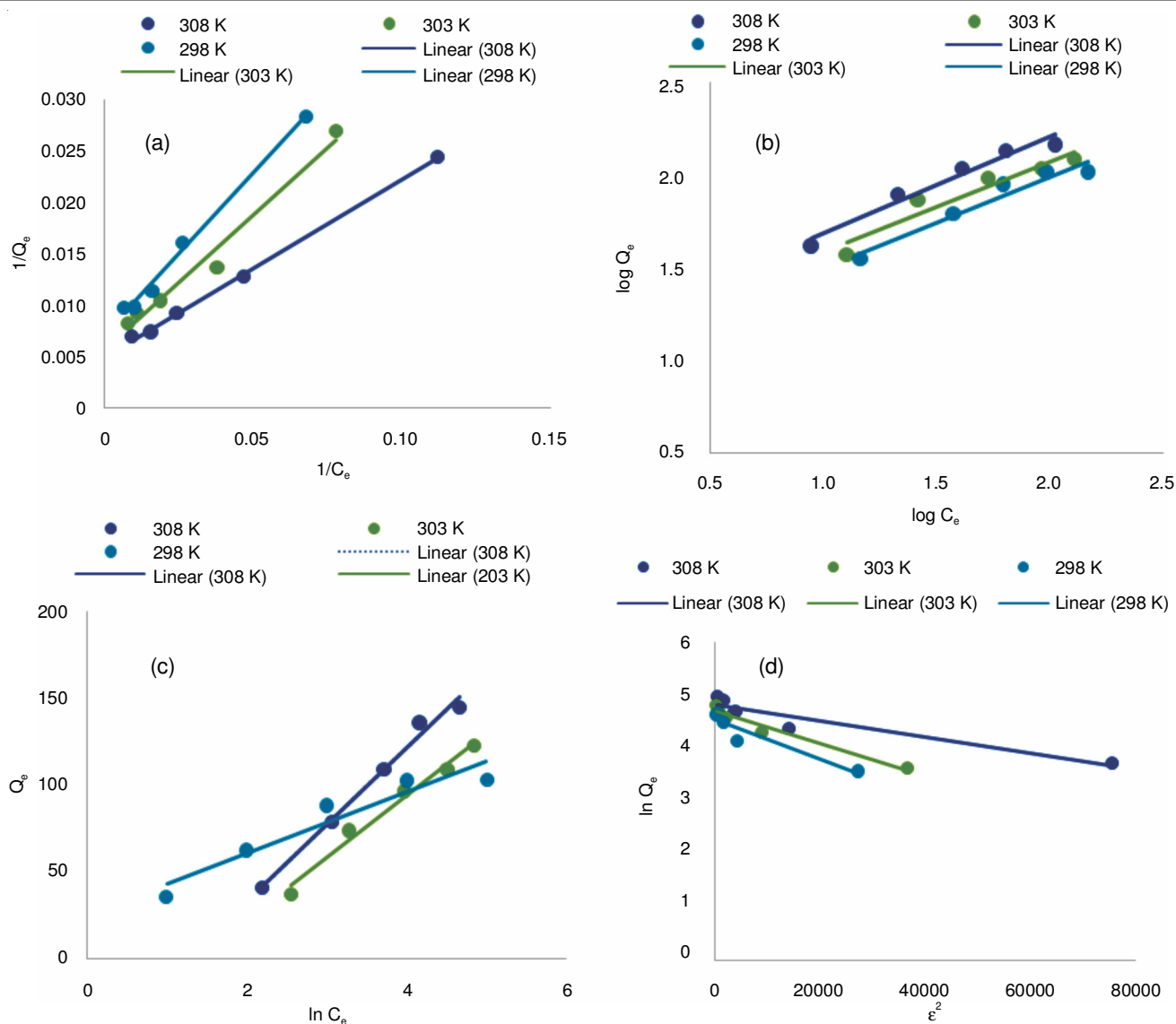


Fig. 10. Graphical representation of various isotherms at different temperatures as (a) Langmuir isotherm, (b) Freundlich isotherm, (c) Temkin isotherm and (d) Dubinin-Radushkevich isotherm (D-R)

TABLE-2  
CALCULATED VALUES OF DIFFERENT CONSTANTS IN VARIOUS ISOTHERMS WITH SDS COATED ZINC FERRITE

Adsorption isotherm	Adsorption behaviour	Linear form	Constants	298 K	303 K	308 K
Langmuir isotherm	Monolayer homogenous	$\frac{1}{Q_e} = \frac{1}{Q} + \frac{1}{bQC_e}$	Q	135.510	170.648	188.324
			B	0.024	0.227	0.032
			R <sup>2</sup>	0.990	0.977	0.992
			SD	0.000800	0.001220	0.000690
Freundlich isotherm	Heterogeneous surface	$\log Q_e = \log K_f + \frac{1}{n} \log C_e$	K <sub>f</sub>	12.825	14.600	19.513
			1/n	0.425	0.442	0.426
			R <sup>2</sup>	0.897	0.901	0.875
			SD	0.067	0.071	0.083
Temkin isotherm	Heat of adsorption is linear rather than logarithmic in nature	$Q_e = \frac{RT}{b} \ln A + \frac{RT}{b} \ln C_e$	b	89.807	75.396	69.450
			A	0.276	0.289	0.429
			R <sup>2</sup>	0.924	0.975	0.912
			SD	8.590	5.937	13.480
Dubnin-Radushkevich isotherm	Porosity adsorption behaviour	$\ln Q_e = \ln Q_m - K \epsilon^2$ $\epsilon = RT \ln \left( 1 + \frac{1}{C_e} \right)$ $E = 1 / \sqrt{(2K)}$	Q <sub>m</sub>	93.682	109.274	124.614
			K	0.00004	0.00003	0.000015
			R <sup>2</sup>	0.893	0.961	0.902
			SD	0.171	0.109	0.186
			E	115.62	128.25	180.78

TABLE-3  
CALCULATED THERMODYNAMIC PARAMETERS FROM VANT HOFF EQUATION

Concentration (mg/L)	$\Delta H$ (KJ/mol)	$\Delta S$ (KJ/mol/K)	$\Delta G$ (298 K)	$\Delta G$ (303 K)	$\Delta G$ (308 K)
50	87.05589	0.300086	-3.26985	-4.77027	-6.2707
100	60.06366	0.208108	-2.57677	-3.61731	-4.65784
150	45.93818	0.158739	-1.84232	-2.63602	-3.42972
200	44.15898	0.148671	-0.59098	-1.33433	-2.07769
250	31.78276	0.103759	0.551384	0.032591	-0.4862
300	22.99902	0.072823	1.079248	0.715132	0.351016

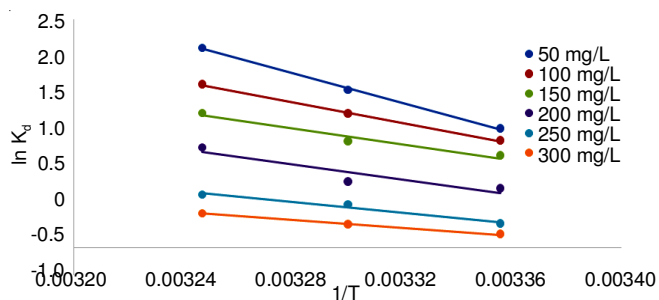


Fig. 11. Vant Hoff plot at different concentration of dye with varying temperature

**Mechanism of Zn ferrite:** It is supposed that zinc ferrite nano particles are neutral in nature and have not much attraction toward cationic and anionic dyes. SDS surfactant is anionic in nature and SDS modified zinc ferrites provide anionic sites at the surface of ZFN which can be used for the adsorption of cationic dyes. This also increases selectivity of the adsorbent. Fig. 12 represents the systematic mechanism of surface modification of ZFN with anionic SDS surfactant for the adsorption of crystal violet dye which is cationic in nature. In step I, when the surfactant concentration is very low then the surfactant moieties are adsorbed to the neutral surface of zinc ferrite. Thus the diffusion of SDS molecules on the surface of zinc

ferrites leads to accumulate negative ions on the surface. In next step, there involves a strong interaction between alkyl tails of anionic surfactant and cationic dye molecules. These hydrophobic interactions between the surfactant molecules and dye molecules are involved the adsorption of dye on the surface of SDS-ZFN.

### Conclusion

This study involves the synthesis of spinel nano zinc ferrite (ZFN) adsorbent with low temperature combustion method and surface modification of nano ferrites with SDS surfactant. Surface characterization and morphological studies of ZFN and ZFN-SDS revealed that these nano particles have good crystalline spinel structure. The experimental data obtained from the study revealed that the ZFN-SDS have excellent ability for the removal of crystal violet dye from water over a wide range of concentrations of dye. The adsorption kinetics of the dye was found to be fitted best to Lagergren pseudo second order kinetic than other models. Various adsorption isotherms studies revealed that Langmuir adsorption isotherm fitted better than other isotherms and indicated that the surface of ZFN-SDS have homogenous in nature. The calculated thermodynamic parameter values such as  $\Delta G^\circ$  was negative indicated the spontaneity of reaction, positive value of  $\Delta H^\circ$

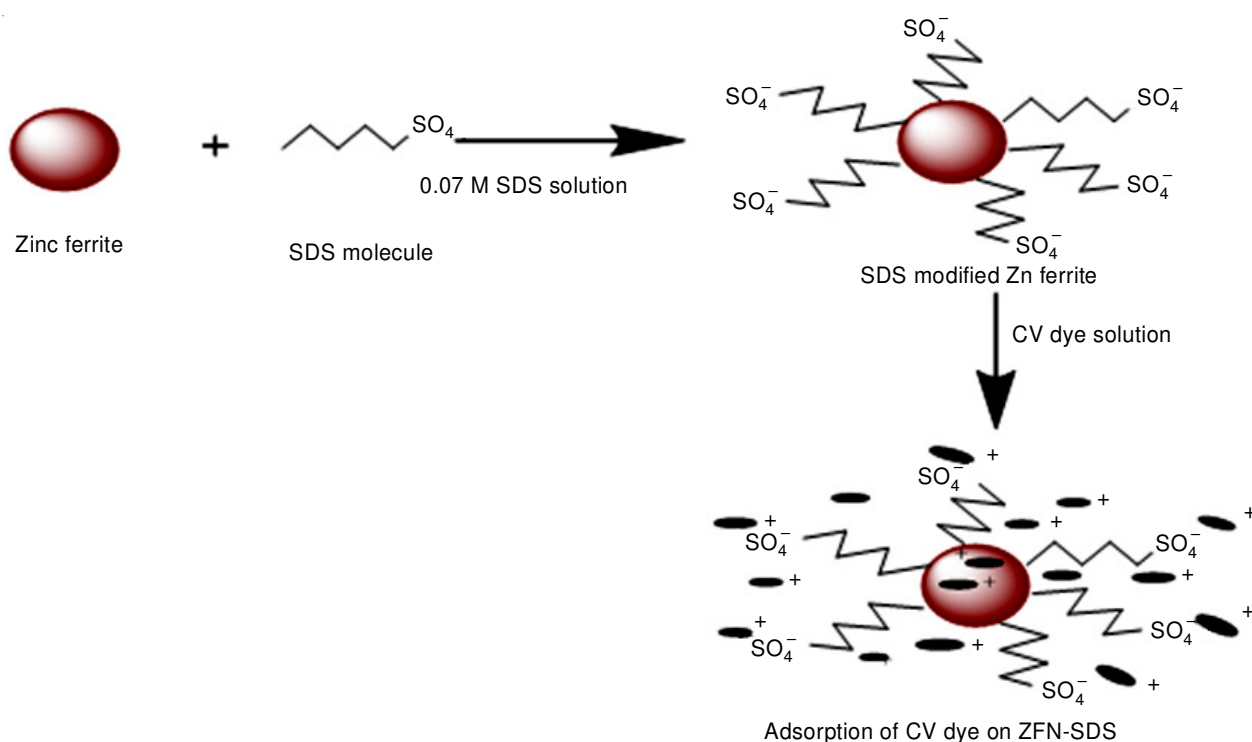


Fig. 12. General mechanism of surface modification of zinc ferrite and dye removal from wastewater



verified the endothermic nature of adsorption and positive value of  $\Delta S^\circ$  showed the increase in degree of freedom of reacting molecules. From above experimental results it can be concluded that ZFN-SDS being as magnetic adsorbent with high dye adsorption capacity might be suitable alternative to remove coloured dyes from waste water.

## REFERENCES

1. T. Robinson, G. McMullan, R. Marchant and P. Nigam, *Bioresour. Technol.*, **77**, 247 (2001); [https://doi.org/10.1016/S0960-8524\(00\)00080-8](https://doi.org/10.1016/S0960-8524(00)00080-8).
2. Ratna and B.S. Padhi, *Int. J. Environ. Sci.*, **3**, 940 (2012); <https://doi.org/10.6088/ijes.2012030133002>.
3. F. Sher, A. Malik and H. Liu, *J. Environ. Chem. Eng.*, **1**, 684 (2013); <https://doi.org/10.1016/j.jece.2013.07.003>.
4. S. Sharma, J.P. Ruparelia and M.L. Patel, A General Review on Advanced Oxidation Processes for Wastewater Treatment, Nirma University International Conference, Ahmedabad, India (2011).
5. J.J. Porter, *Am. Dyest. Report.*, **22**, 21 (1990).
6. S. Mondal and S.R. Wickramasinghe, *J. Membr. Sci.*, **322**, 162 (2008); <https://doi.org/10.1016/j.memsci.2008.05.039>.
7. N.M. Rashed, Adsorption Technique for the Removal of Organic Pollutants from Water and Wastewater, In: Organic Pollutants-Monitoring, Risk and Treatment, Chap. 7, pp. 167-194, INTECH Open Access Publisher (2013); <https://doi.org/10.5772/54048>.
8. J. Qu, *J. Environ. Sci.*, **20**, 1 (2008); [https://doi.org/10.1016/S1001-0742\(08\)60001-7](https://doi.org/10.1016/S1001-0742(08)60001-7).
9. H.A. Hegazi, *HBRC J.*, **9**, 276 (2013); <https://doi.org/10.1016/j.hbrj.2013.08.004>.
10. R. Asakura, M. Morita, K. Maruyama, H. Hatori and Y. Yamada, *J. Mater. Sci.*, **39**, 201 (2004); <https://doi.org/10.1023/B:JMSE.0000007745.62879.74>.
11. M. Soleimani and T. Kaghazchi, *Adv. Chem. Eng. Res.*, **3**, 34 (2014).
12. A.A. Bagreev, A.P. Broshnik, V.V. Strelko and Y.A. Tarasenko, *Russ. J. Appl. Chem.*, **74**, 205 (2001); <https://doi.org/10.1023/A:1012757730582>.
13. H. Zhang, Y. Yan and L. Yang, *Adsorption*, **16**, 161 (2010); <https://doi.org/10.1007/s10450-010-9214-5>.
14. S.L. Liu, Y.N. Wang and K.T. Lu, *J. Porous Mater.*, **21**, 459 (2014); <https://doi.org/10.1007/s10934-014-9792-9>.
15. X. Han, Y. He, H. Zhao and D. Wang, *Korean J. Chem. Eng.*, **31**, 1810 (2014); <https://doi.org/10.1007/s11814-014-0103-6>.
16. F. Ferrero, *Clean Technol. Environ. Policy*, **17**, 1907 (2015); <https://doi.org/10.1007/s10098-015-0908-y>.
17. H. Zeng and S. Sun, *Adv. Funct. Mater.*, **18**, 391 (2008); <https://doi.org/10.1002/adfm.200701211>.
18. K. Okuyama, W. Lenggoro and T. Iwaki, Nanoparticle Preparation and its Application-A Nanotechnology Particle Project in Japan, In: MEMS, NANO and Smart Systems: ICMENS; Proceedings of International Conference on IEEE, pp. 369-372 (2004).
19. D.K. Tiwari, J. Behari and P. Sen, *World Appl. Sci. J.*, **3**, 417 (2008).
20. S. Chaturvedi, P.N. Dave and N.K. Shah, *J. Saudi Chem. Soc.*, **16**, 307 (2012); <https://doi.org/10.1016/j.jscs.2011.01.015>.
21. X. Qu, P.J.J. Alvarez and Q. Li, *Water Res.*, **47**, 3931 (2013); <https://doi.org/10.1016/j.watres.2012.09.058>.
22. M. Mohapatra and S. Anand, *Int. J. Eng. Sci. Technol.*, **2**, 127 (2010); <https://doi.org/10.4314/ijest.v2i8.63846>.
23. B.I. Kharisov, H.R. Dias and O.V. Kharissova, *Arab. J. Chem.*, (2014); <https://doi.org/10.1016/j.arabjc.2014.10.049>.
24. S. An, X. Liu, L. Yang and L. Zhang, *Chem. Eng. Res. Des.*, **94**, 726 (2015); <https://doi.org/10.1016/j.cherd.2014.10.013>.
25. M.P. Tsvetkov, K.L. Zaharieva, Z.P. Cherkezova-Zheleva, M.M. Milanova and I.G. Mitov, *Bul. Chem. Commun.*, **47**, 354 (2015).
26. R.S. Raveendra, P.A. Prashanth, R. Hari Krishna, N.P. Bhagya, B.M. Nagabhushana, H.R. Naika, K. Lingaraju, H. Nagabhushana and B.D. Prasad, *J. Asian Ceram. Soc.*, **2**, 357 (2014); <https://doi.org/10.1016/j.jascer.2014.07.008>.
27. T. Soltani and M.H. Entezari, *J. Mol. Catal. Chem.*, **377**, 197 (2013); <https://doi.org/10.1016/j.molcata.2013.05.004>.
28. M.F. Attallah, I.M. Ahmed and M.M. Hamed, *Environ. Sci. Pollut. Res. Int.*, **20**, 1106 (2013); <https://doi.org/10.1007/s11356-012-0947-4>.
29. M. Faraji, Y. Yamini and M. Rezaee, *J. Iran. Chem. Soc.*, **7**, 1 (2010); <https://doi.org/10.1007/BF03245856>.
30. M. Yu, S. Zhao, H. Wu and S. Asuha, *J. Porous Mater.*, **20**, 1353 (2013); <https://doi.org/10.1007/s10934-013-9721-3>.
31. R. Liu, H. Fu, H. Yin, P. Wang, L. Lu and Y. Tao, *Powder Technol.*, **274**, 418 (2015); <https://doi.org/10.1016/j.powtec.2015.01.045>.
32. S. Jauhar, M. Dhiman, S. Bansal and S. Singhal, *J. Sol-Gel Sci. Technol.*, **75**, 124 (2015); <https://doi.org/10.1007/s10971-015-3682-8>.
33. S.X. Zhang, H.Y. Niu, Y.Q. Cai, X. Zhao and Y.L. Shi, *Chem. Eng. J.*, **158**, 599 (2010); <https://doi.org/10.1016/j.cej.2010.02.013>.
34. R. Sivashankar, A.B. Sathya, K. Vasantharaj and V. Sivasubramanian, *Environ. Nanotechnol. Monitor. Manage.*, **1-2**, 36 (2014); <https://doi.org/10.1016/j.enmm.2014.06.001>.
35. M.R. Patil and V.S. Shrivastava, *Pelagia Res. Libr.*, **5**, 8 (2014).
36. Z. Li, M.A. Gondal and Z.H. Yamani, *J. Saudi Chem. Soc.*, **18**, 208 (2014); <https://doi.org/10.1016/j.jscs.2011.06.012>.
37. M.A. Gabal, E.A. Al-Harthy, Y.M. Al-Angari and M.A. Salam, *Chem. Eng. J.*, **255**, 156 (2014); <https://doi.org/10.1016/j.cej.2014.06.019>.
38. S. Hashemian, *Afr. J. Biotechnol.*, **9**, 8667 (2010); <https://doi.org/10.5897/AJB09.1296>.
39. E. Alzahrani, *Int. J. Innov. Res. Sci. Eng. Technol.*, **3**, 15118 (2014); <https://doi.org/10.15680/IJIRSET.2014.0308009>.
40. N.M. Mahmoodi, J. Abdi and D. Bastani, *J. Environ. Health Sci. Eng.*, **12**, 96 (2014); <https://doi.org/10.1186/2052-336X-12-96>.
41. M.R. Patil and V.S. Shrivastava, *Appl. Nanosci.*, **5**, 809 (2015); <https://doi.org/10.1007/s13204-014-0383-5>.
42. M.R. Patil, S.D. Khairnar and V.S. Shrivastava, *Appl. Nanosci.*, **6**, 495 (2016); <https://doi.org/10.1007/s13204-015-0465-z>.
43. Y. Xiao, H. Liang, W. Chen and Z. Wang, *Appl. Surf. Sci.*, **285**, 498 (2013); <https://doi.org/10.1016/j.apsusc.2013.08.083>.
44. C. Li, Y. Dong, J. Yang, Y. Li and C. Huang, *J. Mol. Liq.*, **196**, 348 (2014); <https://doi.org/10.1016/j.molliq.2014.04.010>.
45. Y. Li, Y. Zhou, W. Nie, L. Song and P. Chen, *J. Porous Mater.*, **22**, 1383 (2015); <https://doi.org/10.1007/s10934-015-0017-7>.
46. H. Jiang, P. Chen, S. Luo, X. Luo, X. Tu, Q. Cao, Y. Zhou and W. Zhang, *J. Inorg. Organomet. Polym. Mater.*, **23**, 393 (2013); <https://doi.org/10.1007/s10904-012-9792-7>.
47. Q. Lian, Y. Cui, X. Zheng and H. Wu, *Russ. J. Appl. Chem.*, **88**, 1877 (2015); <https://doi.org/10.1134/S10704272150110208>.
48. M. Singh, H.S. Dosanjh and H. Singh, *J. Water Process. Eng.*, **11**, 152 (2016); <https://doi.org/10.1016/j.jwpe.2016.05.006>.
49. N. Dalali, M. Khoramnezhad, M. Habibizadeh and M. Faraji, International Conference on Environmental, Agriculture and Engineering, IPCBEE, Singapore (2011).
50. N.M. Mahmoodi, *J. Ind. Eng. Chem.*, **27**, 251 (2015); <https://doi.org/10.1016/j.jiec.2014.12.042>.